



**HAL**  
open science

## Porous granules by freeze granulation of Pickering emulsions stabilized with halloysite particles

M. Ouadaker, X. Jiang, P. Bowen, M. Bienia, C. Pagnoux, A. Aimable

### ► To cite this version:

M. Ouadaker, X. Jiang, P. Bowen, M. Bienia, C. Pagnoux, et al.. Porous granules by freeze granulation of Pickering emulsions stabilized with halloysite particles. *Colloids and Surfaces A: Physicochemical and Engineering Aspects*, 2020, 585, pp.124156. 10.1016/j.colsurfa.2019.124156 . hal-02469334

**HAL Id: hal-02469334**

<https://unilim.hal.science/hal-02469334v1>

Submitted on 21 Jul 2022

**HAL** is a multi-disciplinary open access archive for the deposit and dissemination of scientific research documents, whether they are published or not. The documents may come from teaching and research institutions in France or abroad, or from public or private research centers.

L'archive ouverte pluridisciplinaire **HAL**, est destinée au dépôt et à la diffusion de documents scientifiques de niveau recherche, publiés ou non, émanant des établissements d'enseignement et de recherche français ou étrangers, des laboratoires publics ou privés.



Distributed under a Creative Commons Attribution - NonCommercial 4.0 International License

# Porous granules by freeze granulation of Pickering emulsions stabilized with halloysite particles

M. Ouadaker<sup>(1)</sup>, X. Jiang<sup>(2)</sup>, P. Bowen<sup>(2)</sup>, M. Bienia<sup>(1)</sup>, C. Pagnoux<sup>(1)</sup>, A. Aimable<sup>(1)\*</sup>

(1) Univ. Limoges, CNRS, IRCER, UMR 7315, F-87000 Limoges, France

(2) Laboratory of Construction Materials (LMC), Swiss Federal Institute of Technology EPFL, 1015, Lausanne, Switzerland

\* Corresponding author:

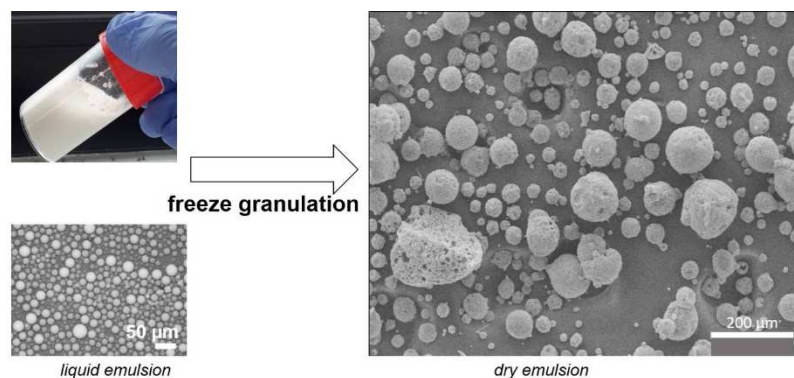
Anne Aimable

E-mail : [anne.aimable@unilim.fr](mailto:anne.aimable@unilim.fr)

Phone : +33 (0) 587 50 23 68

Fax : +33 (0) 587 50 23 04

## Graphical abstract



## Abstract

Pickering emulsions stabilized with a natural silicate mineral, halloysite, were dried by freeze granulation in order to prepare porous granules. Different formulations were studied, by varying the pH of the suspension, the ionic strength and with the addition of organic binders (poly(vinyl alcohol) (PVA) and poly(ethylene glycol) (PEG)). To get a better understanding and control on the process the objective was to correlate the formulation and the emulsion behavior to the morphology and size of the granules. This study highlights the predominant role of electrostatic interactions on the emulsions. Their stability is improved if the dispersion of solid particles in the continuous phase is relatively limited, with medium zeta potential absolute values. Freeze granulation of emulsions prepared at different ionic strength and pH led to similar granules,

27 with an internal porosity attributed to the low solid fraction. The addition of organic additives  
28 PVA and PEG led to a better conservation of the structure, with fewer broken fragments and a  
29 larger porosity, attributed to a higher cohesion of these emulsions during the spray freezing  
30 and the lyophilisation steps.

31

## 32 **Keywords**

33 Pickering emulsion; freeze granulation; lyophilisation; halloysite; porosity; rheology

34

## 35 **1- Introduction**

36 Pickering emulsions are emulsions stabilized by solid particles adsorbing at the liquid/liquid  
37 interface [1]. They were first described by Ramsden [2] and Pickering [3]. They are employed  
38 in many different fields, such as cosmetics, paints, food industry, or coal treatments. They  
39 present a very long shelf life and a strong resistance to coalescence attributed to a non-  
40 reversible attachment of solid particles at the oil-water interface. This mechanism was  
41 extensively supported by a theoretical approach and thermodynamic calculations, described  
42 in many publications [4][5][6][7]. The type of emulsion is determined by the particle wettability  
43 at the oil-water interface: hydrophilic particles lead to the dispersion of the oil phase in the  
44 aqueous medium (O/W), whereas hydrophobic particles to the dispersion of the aqueous  
45 phase (W/O) [8]. Surface properties are generally modified, either by organic species  
46 adsorption or chemical grafting, to enhance emulsion stability [9][10][11][12][13]. However  
47 stabilization of emulsions without additives is a real challenge, especially for cosmetic and food  
48 applications, where lowering the amount of chemicals is of great benefit for the health of the  
49 consumers. The use of clay minerals such as montmorillonite [14], mica [15], hectorite and  
50 bentonite [16], or laponite [17] was reported in the literature. The stabilization of Pickering  
51 emulsions without surface modification is possible because their chemistry and the layer  
52 structure allow them to have amphiphilic properties [18]. In that context, clays offer a great  
53 opportunity for the development of surfactant-free emulsions. Moreover they are readily  
54 available, cheap and natural resources.

55 In a previous study, we compared kaolin, halloysite and palygorskite as Pickering emulsion  
56 stabilizer [19]. All three phyllosilicates led to stable emulsions at high solid contents (15 wt.%  
57 equal to 5.0 vol.% in the aqueous phase) without any surface modification. They showed  
58 different rheological behaviors, halloysite leading to the highest cohesion of the emulsion,  
59 which was attributed to its higher specific surface area.

60 In the present study the aim was to prepare porous granules from Pickering emulsions of  
61 halloysite via freeze granulation. This process consists of an atomization into small droplets of  
62 a suspension or an emulsion through a spraying nozzle [20]. Droplets are sprayed into liquid  
63 nitrogen under stirring and are instantly frozen. The resulting frozen granules are recovered  
64 and subsequently freeze-dried under vacuum to sublimate the ice they contain and yield a dry  
65 granulated powder. Compared to the spray-drying process [21][22], freeze granulation leads  
66 to a better control of granule density and a higher homogeneity. Indeed, droplet freezing is a  
67 fast process, and lyophilisation prevents shrinkage and deformations generally observed  
68 during the drying step (such as the doughnut effect). This technology presents the great  
69 advantage to preserve the structure and homogeneity of the particles in suspension [23]. It is  
70 suitable for the preparation of fine powders, re-dispersible formulations, nanomaterials, drug  
71 delivery systems, etc... Organic compounds, pharmaceutical products or other heat sensitive  
72 materials benefit from this low temperature and low pressure process. Technical ceramics  
73 such as transparent ceramics [24][25], MOX fuels [26] or non-oxide ceramics [27][28][29] have  
74 also been prepared with high performances.

75 Freeze granulation was chosen for its ability to retain the structure of the slurry. The aim was  
76 to investigate if an O/W Pickering emulsion could lead to the formation of macroporous  
77 granules made of ceramic materials after elimination of the liquid phases. If there are many  
78 papers published on processing routes based on Pickering emulsions, most of them deal with  
79 organic materials. Macroporous ceramic materials are obtained by processing routes generally  
80 classified into replica, sacrificial template, and direct foaming methods [30]. However some  
81 groups have reported on particle-stabilized emulsions as templates for the fabrication of  
82 porous materials [10][31][32]. More recently additive manufacturing such as extrusion-based  
83 3D printing also succeeded in the fabrication of hierarchical porous materials, leading to very  
84 well-designed and complex geometries [33][34][35]. A large range of applications exist for such  
85 macroporous ceramic materials such as drug delivery systems, chemical containers, or  
86 catalyst supports.

87 Therefore different formulations of emulsions were studied, by varying the pH of the  
88 suspension, the ionic strength and with the addition of organic binders (poly(vinyl alcohol)  
89 (PVA) and poly(ethylene glycol) (PEG)). Through this study we tried to get a better  
90 understanding and control on the process by making correlations between the formulation, the  
91 emulsion behavior and the morphology and size of the materials obtained by freeze  
92 granulation.

93

94

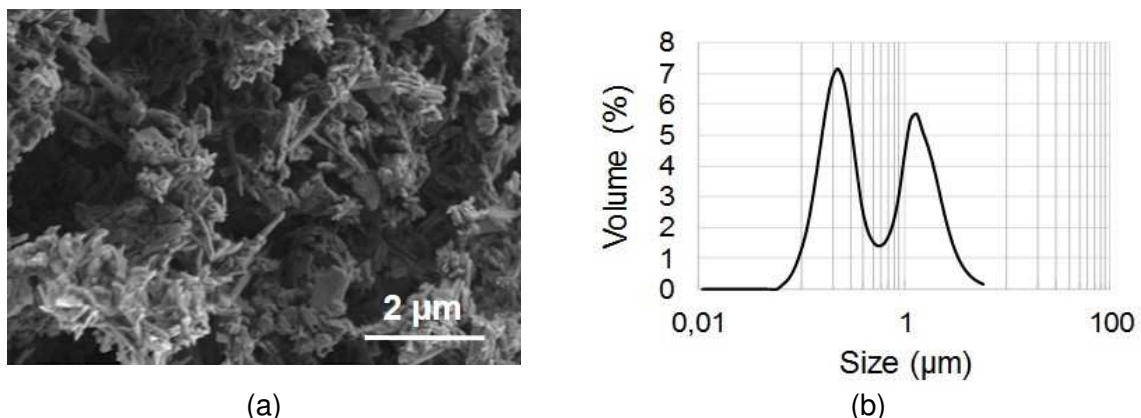
95 **2- Experimental section**

96 **2.1 Raw materials**

97 Halloysite powder is provided by Imerys Ceramics under the name Premium NZCC. This clay  
98 is a phyllosilicate with the formula  $\text{Al}_2\text{Si}_2\text{O}_5(\text{OH})_4 \cdot n\text{H}_2\text{O}$ ,  $n$  being comprised between 0 and 2.  
99 Halloysite is a dioctahedral 1:1 clay mineral of the kaolin group and has a multilayer tubular  
100 structure. This structure results from the wrapping of the 1:1 clay mineral layers, driven by a  
101 mismatch in the oxygen-sharing tetrahedral and octahedral sheets in the 1:1 layer. Halloysite  
102 is chemically similar to kaolin, but the unit layers are separated by a layer of water molecules.  
103 This gives a remarkable surface chemistry of halloysite: the external surface of the tubes is  
104 composed of Si–O–Si groups, whereas the internal lumen surface consists of a gibbsite-like  
105 array of Al–OH groups [36][37][38]. This lead to different surface charges of the materials  
106 depending on the pH.

107 Halloysite presents an elongated tubular morphology, with a width around 100 nm and a length  
108 of 1-2  $\mu\text{m}$ . The morphology of the particles is visible in the SEM image (Figure 1a), and Figure  
109 1b shows the particle size distribution of halloysite measured by laser diffraction, which is  
110 bimodal, corresponding to the two sizes (width and length) of particles, expected for platelet  
111 like particles with such a large difference between thickness and length [39], as well as a small  
112 agglomeration of these particles.

113



114 Figure 1: (a) SEM image of halloysite, (b) Particle size distribution of halloysite by laser  
115 granulometry (in diluted aqueous suspension, natural pH)

116

117 Halloysite density was taken at 2.8  $\text{g}/\text{cm}^3$ . Halloysite was dispersed into deionized water, or  
118 NaCl solutions at different concentrations (prepared from NaCl 99%, Aldrich). Dodecane  
119 ( $\text{C}_{12}\text{H}_{26}$ , Sigma-Aldrich, density = 0.75  $\text{g}/\text{cm}^3$ ) was used without further treatment as the oil  
120 phase.

121 PVA (poly(vinyl alcohol), Mw = 25000g/mol) and PEG (poly(ethylene glycol), Mw = 300g/mol)  
122 from Aldrich were used respectively as binder and plasticizer to increase the cohesion of the  
123 final powder during the freeze granulation process.

124

## 125 **2.2 Emulsion preparation procedure**

126 Emulsions are obtained by mixing aqueous suspensions of halloysite with dodecane. In a  
127 typical formulation, halloysite particles were introduced into the water at the volume fraction  
128 5.0 vol.%. This suspension was stirred magnetically at 500 rpm during two minutes, and  
129 dispersed using an ultrasonic pulsing method (3s On, 1s Off) during two minutes. Then  
130 dodecane was added at a ratio R corresponding to the volume ratio of dodecane to water of  
131 0.44 (defined by a previous study [19]). A high-shear stirring was applied at 19000 rpm during  
132 two minutes with an Ultra-Turrax T25 homogenizer in order to form the emulsion.

133 To study the effect of the pH, NaOH (0.1M) solution was introduced into the suspension  
134 (natural pH = 3.4) controlled using a pH-meter.

135 To study the effect of the ionic strength of the suspension, NaCl solutions at different known  
136 concentrations were used instead of water.

137 In order to increase the cohesion of the material during the freeze granulation processing step,  
138 a mixture of polymers, PVA and PEG, was also added at different concentrations. They were  
139 previously diluted in water, and introduced into the suspension to the desired concentration  
140 prior to the emulsification step.

141

## 142 **2.3 Freeze granulation of halloysite stabilized emulsions**

143 The main objective of this study was to dry Pickering emulsions of halloysite by freeze  
144 granulation. This operation follows two stages: the first is spray freezing, and the second is  
145 freeze drying (or lyophilization).

146 Spray freezing consists of spraying a suspension (here an emulsion) with compressed air into  
147 a large volume (around 1 liter) of liquid nitrogen, in order to form granules by an instantaneous  
148 freezing of the fluid droplets. The rapid freezing allows the conservation of the spherical shape  
149 created by spraying through the nozzles. The freeze granulator (LS-2, PowderPro AB) is  
150 equipped with a suspension flow regulating device provided with the apparatus. The atomizer  
151 used was of the twin-fluid nozzle type. Both air and suspension inlets had inner diameters of 4  
152 mm and the droplet spraying outlet had an inner diameter of 1 mm. The atomization gas used  
153 was air. Unless otherwise stated, the atomization conditions performed were: air relative  
154 pressure of 0.2 bar and suspension flow rate of 33 mL/min (suspension pumped through a  
155 peristaltic pump). The rotation speed of the magnetic stirrer in the liquid nitrogen was set at  
156 350 rpm. Immediately after formation, frozen granules were freeze dried in a Christ Alpha 2–4

157 LD Plus freeze-drier. Freeze drying aims at removing the liquid phase present in the frozen  
158 suspension or emulsion granules by sublimation. This procedure lasts about 20 hours to  
159 maintain the structure of the granules after removing the liquid, under a final vacuum of  $10^{-3}$   
160 mbar.

161

## 162 **2.4 Characterization techniques**

163 Zeta potential measurements were conducted on halloysite suspensions (5 vol.%) with an ESA  
164 analyser (AcoustoSizer II S flow through system, Colloidal Dynamics). The zeta potential was  
165 obtained from the ESA voltage data treated with the AcoustoSizer II operation software by  
166 using the O'Brien relationship. Zeta potential measurements were done varying the ionic  
167 strength by NaCl addition, varying pH with 1.0 mol/L sodium hydroxide addition, or with an  
168 addition of PVA and PEG as aqueous solutions at the concentration 10 wt.%, with the  
169 automated AcoustoSizer II pH titration system.

170 The stability, phase separation or creaming of emulsions was characterized **after visual**  
171 **observations.**

172 Emulsion droplets **were observed** using an optical microscope Nikon Eclipse 501. A small  
173 amount of freshly prepared emulsion was placed on a microscope slide, and covered after  
174 ensuring that no air gap or bubbles were trapped between the sample and the cover slip.

175 Laser diffraction analysis was used to determine the droplet size distribution of emulsions  
176 (Horiba LA-950), using the Fraunhofer mode. **Emulsions were analysed in the liquid module,**  
177 **whereas freeze dried granules were analysed in the dry module.**

178 Emulsions were characterized using a stress-controlled rheometer ARG2 from TA Instruments.  
179 The measuring geometry consisted of a 20 mm diameter upper plate and a Peltier lower plate.  
180 The gap was set to 1 mm.

181 The viscous and elastic responses were investigated by dynamic oscillatory tests carried out  
182 at 20 °C. The principle of this measurement is to apply a sinusoidal strain and measure the  
183 corresponding stress. In this procedure the linear viscoelastic region can be detected. The  
184 dynamic response between strain ( $\gamma$ ) and stress ( $\tau$ ) can be described as follows:

$$185 \quad \tau = G^* \gamma \quad (1)$$

186 where  $G^*$  is the complex modulus consisting elastic ( $G'$ ) and viscous ( $G''$ ) components.

187 The relationships are shown below and  $\tan \delta$  is the loss factor which equals to  $G''/G'$ :

$$188 \quad G' = G_0 \cos \delta \quad (2)$$

$$189 \quad G'' = G_0 \sin \delta \quad (3)$$

190 The linear viscoelastic region (LVER) is determined by oscillatory strain sweep from  $10^{-4}$  to 0.1  
191 at a fixed frequency of 1 Hz. The critical elastic modulus ( $G'_c$ ) and critical strain ( $\gamma_c$ ) are obtained



192 from the flow onset point, and the onset point allows us to calculate the cohesive energy  $E_c$   
193 using the equation below:

$$194 \quad E_c = \frac{1}{2} G'_c \gamma_c^2 \quad (4)$$

195 The cohesive energy corresponds to the elastic strength of the material, and thus could be  
196 considered as a measurement of the strength of the internal structure of the emulsion; the  
197 higher the cohesive energy, the more stable a system should be.

198 In order to characterize better the rheological behavior during the pumping operation, steady  
199 state flow measurements were also performed. They consist of a series of creep experiments  
200 with varying stress, where the equilibrium shear rate is obtained when the curve reaches a  
201 linear regime. The stress was varied using the following cycle:

- 202 1. a pre-shear at the maximum shear stress (20 Pa),
- 203 2. a decreasing shear stress sweep,
- 204 3. an increasing shear stress sweep.

205 **The morphology and size of materials** obtained by freeze granulation were observed by  
206 Scanning Electron Microscopy (SEM, Quanta 450 FEG) under vacuum mode (HV: 2 keV,  
207 working distance: 9 mm, spot: 3.0).

208

## 209 **3- Results and discussion**

210

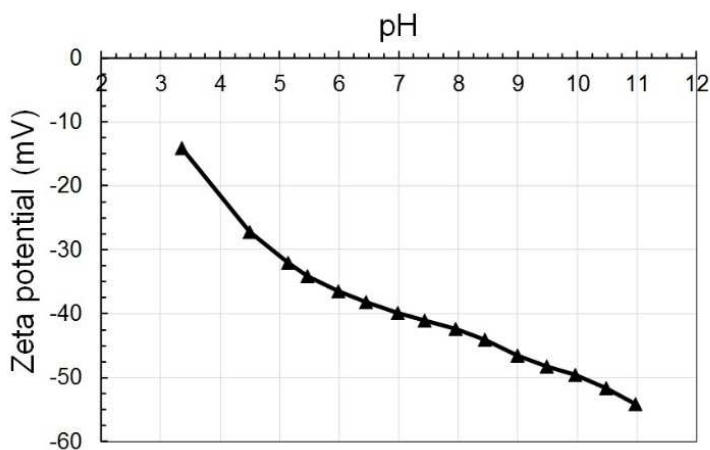
### 211 **3.1- Influence of pH on halloysite suspensions and emulsions**

212 Zeta potential of an halloysite suspension (concentration 5.0 vol.%) was measured as a  
213 function of the pH (Figure 2). Halloysite suspension in deionized water presents a natural pH  
214 value of 3.4 corresponding to a negative zeta potential value of -14 mV. By adding NaOH, the  
215 pH increases and the zeta potential decreases rapidly, to attain -50 mV at pH 10, ensuring a  
216 better dispersion of particles, and thus a better stability of the suspension. The typical tubular  
217 morphology of halloysite is described with the Si-OH groups on the outer surface, whereas the  
218 inner surfaces of the tubes present Al-OH groups [36][37][38]. Therefore the measurement  
219 obtained from the Acoustosizer (which is an average zeta response) is more similar to a silica  
220 material, because of its presence at the external surfaces. Moreover in the acidic pH range,  
221 the inner and the outer surfaces present opposite charges, whereas at basic pH, both surfaces  
222 are negative, leading to higher absolute values.

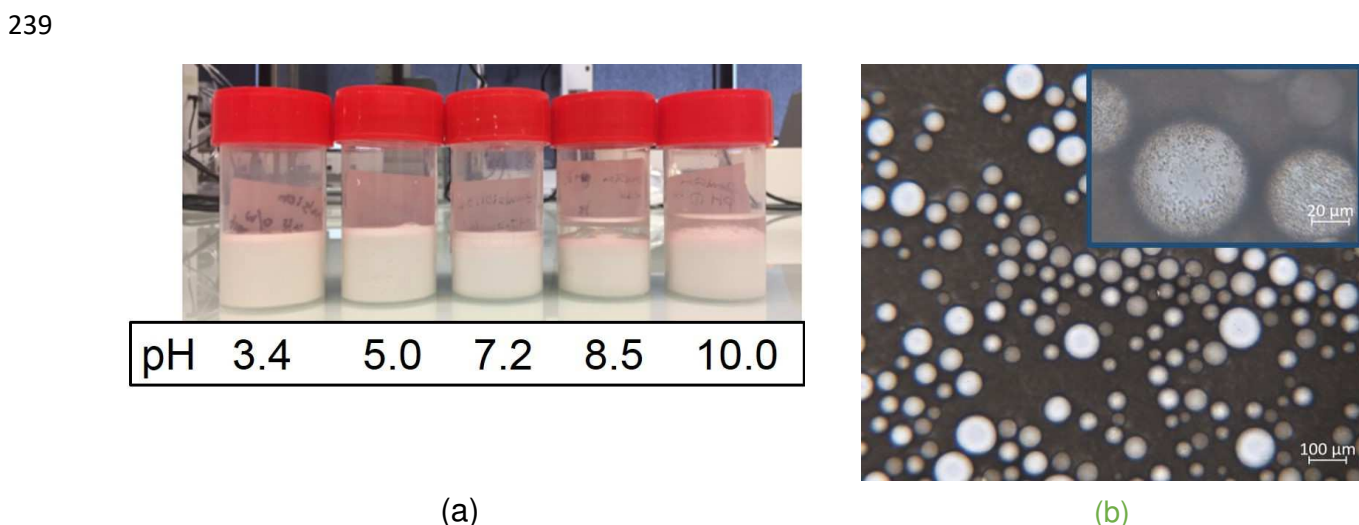
223 **Emulsions were prepared with dodecane at a volume ratio  $R = 0.44$ . A stable O/W emulsion**  
224 **was obtained at the natural pH (Figure 3(a)). Optical microscopy shows that halloysite particles**



225 are located at the O/W interface, but also in the continuous aqueous phase (Figure 3(b)).  
 226 Increasing the pH of the suspension impacted the stability of the emulsion, and creaming was  
 227 rapidly observed at pH > 7.0 (Figure 3(a)). This corresponds to the transition from positive to  
 228 neutral and negative surface charges of the alumina-like surfaces. It has been shown that most  
 229 oil phases present negative surface charges [40][41], therefore repulsive interactions between  
 230 halloysite particles and dodecane increase when pH increases, leading to the emulsion  
 231 breaking. Furthermore a higher zeta potential in absolute value corresponds to a better  
 232 dispersion of halloysite particles in the aqueous phase, which is not favorable for their migration  
 233 at the oil/water interface. To conclude, a high negative surface charge of halloysite particles is  
 234 not recommended to stabilize oil droplets in a Pickering emulsion, whereas a slightly  
 235 flocculated state is more favorable (pH < 6).



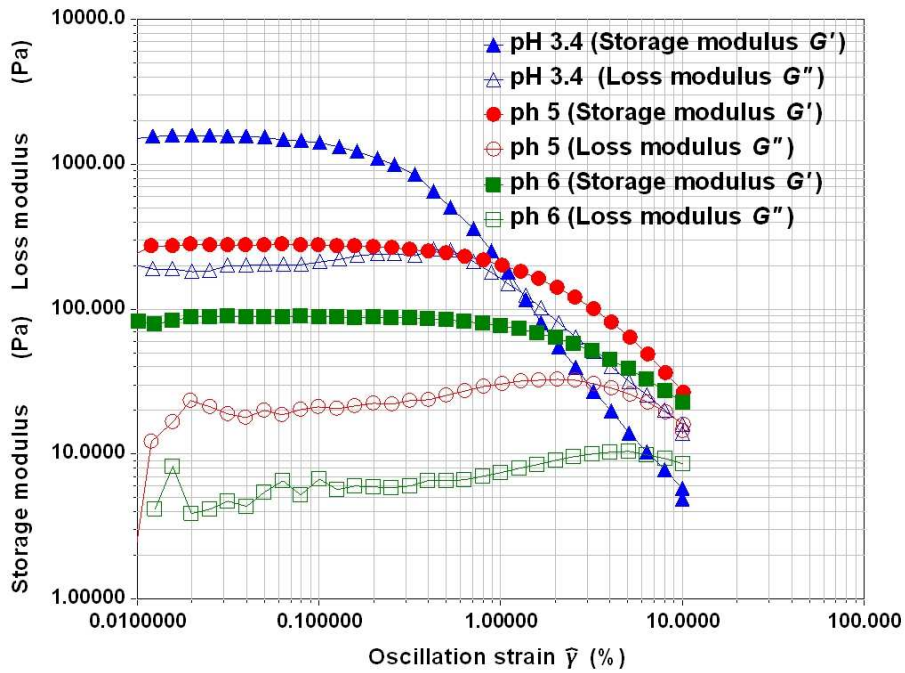
236  
 237 Figure 2: Zeta potential of an halloysite suspension as a function of the pH (volume fraction of  
 238 halloysite 5.0 vol.% in deionized water, natural pH = 3.4)



240 Figure 3: (a) Observations of the stability of Pickering emulsions prepared at different pH, after  
 241 1 week (volume fraction of halloysite 5.0 vol.% in deionized water, O/W ratio = 0.44 in volume),  
 242 (b) O/W emulsion at pH 3.4

243

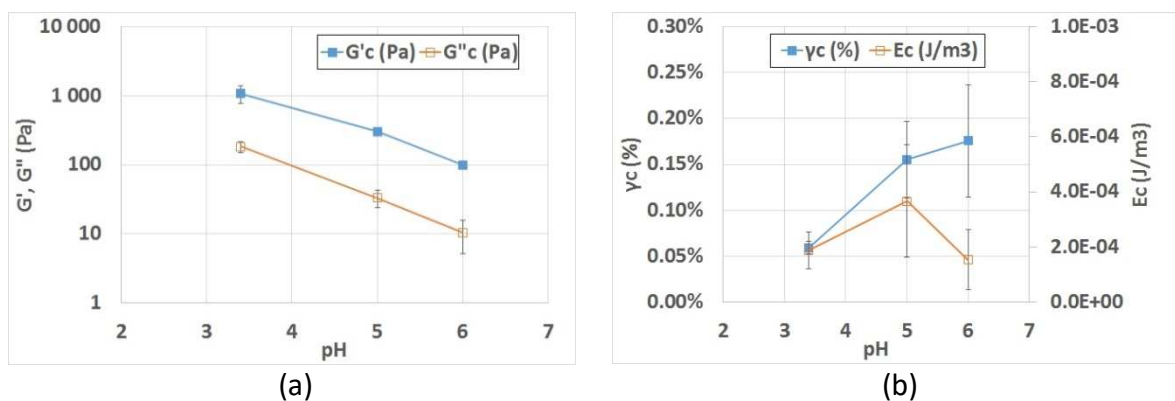
244 Oscillatory measurements have been conducted on relatively stable emulsions, at acidic pH  
245 (from pH 3.4 to pH 6, Figure 4). The elastic (storage) modulus  $G'$  is always superior to the  
246 viscous one (loss modulus)  $G''$ , corresponding to a solid-like behavior (Figure 5a).  $G'$  is the  
247 largest for the case of natural pH. The critical strain increases with pH, whereas the cohesion  
248 energy is similar regarding the large error bars (Figure 5b). Therefore the natural pH  
249 corresponds to the most favorable pH to prepare a Pickering emulsion with halloysite.



250

251 Figure 4: Oscillatory results for halloysite emulsions prepared at different pH

252



253 Figure 5: (a) critical storage modulus  $G'_c$  and critical loss modulus  $G''_c$ , (b) critical strain  $\gamma_c$ , and  
254 cohesive energy  $E_c$ , of halloysite emulsions at different pH

255

256

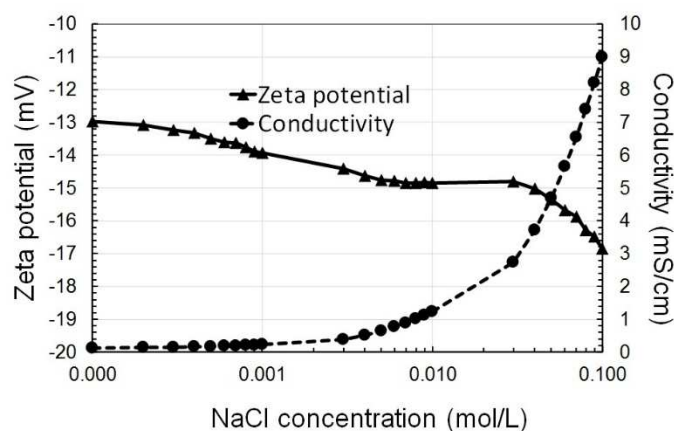
257

### 258 3.2- Influence of NaCl concentration on halloysite suspensions and emulsions

259 Emulsions were prepared with NaCl at different concentrations to vary the ionic strength of  
260 halloysite suspensions. The conductivity evolution was significant, from 0.1 mS/cm without  
261 NaCl, to 1.3 mS/cm for [NaCl] = 0.01 M, and 9 mS/cm for [NaCl] = 0.1 M (Figure 6). However  
262 the stability of the emulsions was not influenced by NaCl concentration, and all emulsions were  
263 stable during several weeks, with no sedimentation neither coalescence nor creaming  
264 observed. From laser diffraction analysis (Figure 7), they all present a similar droplet size  
265 around 80  $\mu\text{m}$ . The rheological behavior is also very similar whatever the NaCl concentration  
266 (Figures 8 and 9). The analysis of the oscillatory measurements gives a critical storage  
267 modulus  $G'_c$  comprised between 800 and 1000 Pa, and the critical loss modulus  $G''_c$  around  
268 200 Pa. The critical deformation  $\gamma_c$  is around 0.06%, which leads to a relatively low cohesive  
269 energy around 0.15 mJ/m<sup>3</sup>.

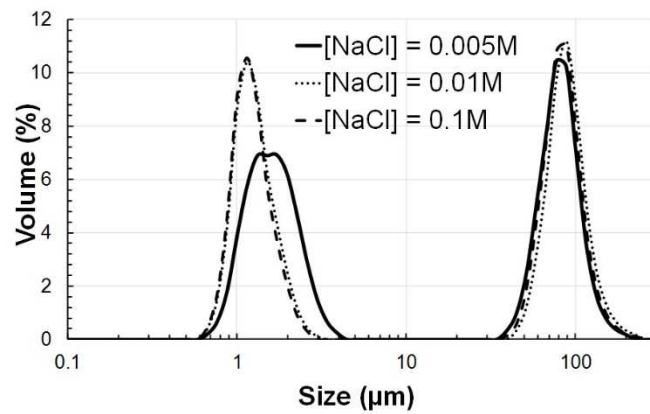
270 **To explain this insensitivity**, zeta potential was measured on halloysite suspensions by varying  
271 NaCl concentrations at a constant pH of 3.4 (natural pH). Zeta potential was also surprisingly  
272 quasi constant whatever NaCl concentration. It slightly decreased from -13 mV to -17 mV  
273 whereas the conductivity of the suspension increased drastically, from 0.1 to 9 mS/cm (Figure  
274 6). In the DLVO theory, a higher conductivity usually leads to a compression of the double  
275 layer of the particles, leading to lower absolute values of zeta potential, and loss of stability.  
276 This is not observed here, with a low impact of NaCl concentration attributed to a low  
277 modification of particle-particle interactions in the suspension. This can be explained if Na<sup>+</sup> and  
278 Cl<sup>-</sup>, which were assumed at first as non-potential determining ions, specifically adsorb on  
279 halloysite surfaces [42]. **This is possible for** halloysite particles, which present a very specific  
280 rolled plate morphology, with silica-like surface in the inner of the tubes, and alumina-like  
281 surface at the outer of the tubes [36][37][38], and therefore can adsorb both ions at acid pH.

282  
283



284  
285 Figure 6: Evolution of zeta potential and conductivity of halloysite suspensions with NaCl  
286 concentrations varying from 0 to 0.1 M (volume fraction of halloysite 5.0 vol.%, natural pH =  
287 3.4 - pH remains constant)

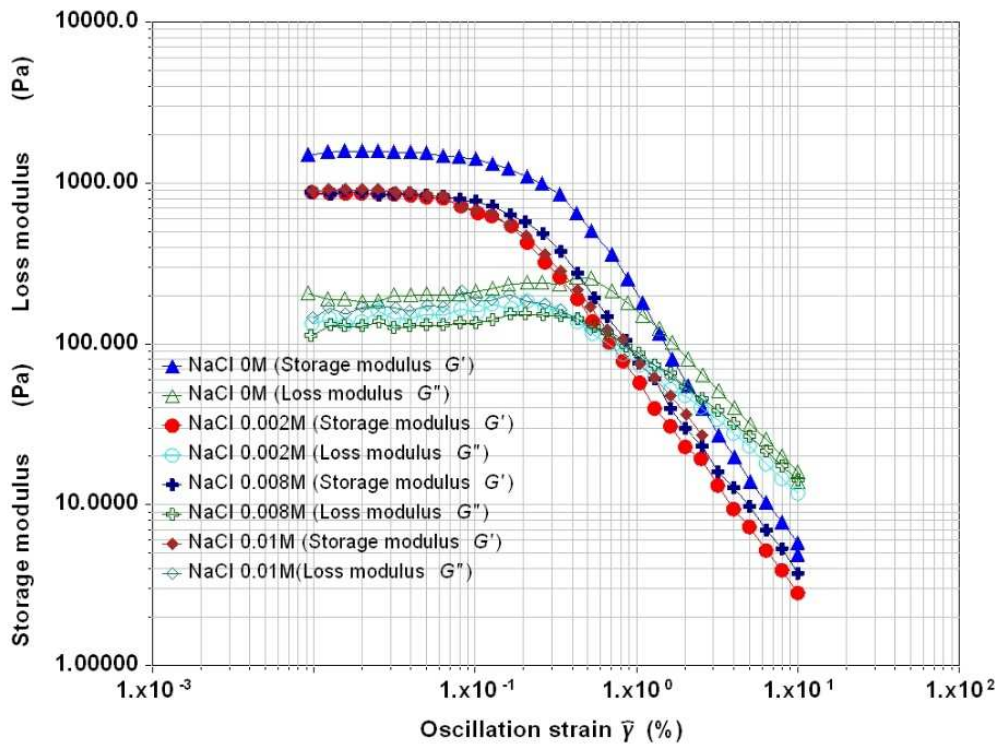
288



289

290 Figure 7: Laser diffraction analysis of halloysite emulsions at different NaCl concentrations and  
291 natural pH

292

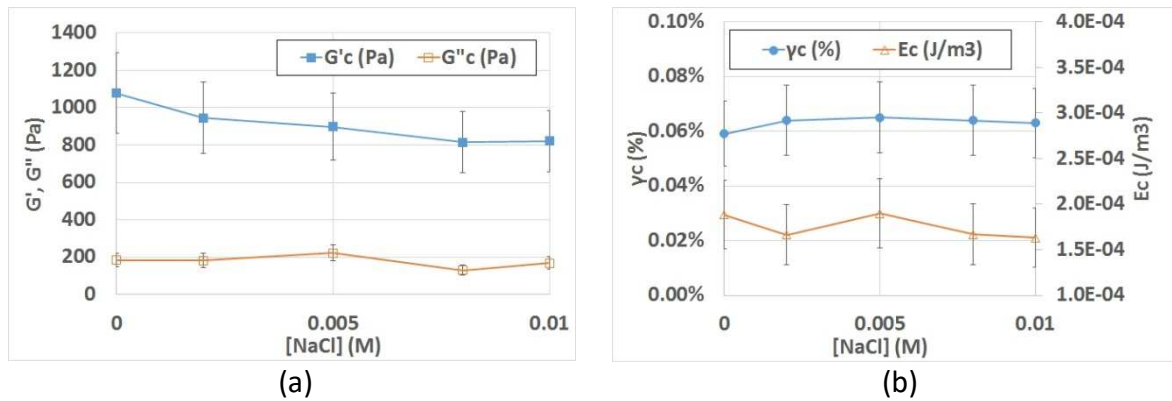


293

294 Figure 8: Oscillatory results G' and G'' for amplitude sweep at 1 Hz of halloysite emulsions at  
295 different NaCl concentration and natural pH

296

297



298

299 Figure 9: (a) critical storage modulus  $G'_c$  and critical loss modulus  $G''_c$ , (b) critical strain  $\gamma_c$ , and  
 300 cohesive energy  $E_c$ , of halloysite emulsions at different NaCl concentration and natural pH  
 301

302 To conclude, these studies with different pH and NaCl concentrations are very informative as  
 303 they highlight the predominant role of electrostatic interactions on the behavior of these  
 304 emulsions. Their stability is improved if the dispersion of solid particles in the continuous phase  
 305 is relatively limited, with medium zeta potential absolute values. Furthermore in this particular  
 306 case, NaCl is not able to modify zeta potential and thus particle interactions, and emulsions  
 307 present similar properties in terms of droplet size, stability, and rheology.

308

### 309 3.3- Influence of addition of binders (PVA and PEG) on halloysite suspensions and 310 emulsions

311 Organics are usually added in ceramic processes in order to improve the processability or the  
 312 handling of green pieces[43]. PVA and PEG were chosen respectively as a binder and a  
 313 plasticizer for increasing the granule cohesion during freeze granulation.

314 At first the influence of PVA and PEG was studied in **halloysite suspensions**. Interfacial  
 315 properties were investigated, because the lower the interfacial energy between two immiscible  
 316 phases, the better it is for emulsification. Table 1 shows that adding halloysite particles at  
 317 natural pH reduces drastically the interfacial energy compared to pure water, from 43 mN/m to  
 318 9 mN/m. This explains the stability of Pickering emulsions with halloysite, these particles alone  
 319 are able to stabilize oil droplets. When adding PEG, the interfacial energy remains as low as  
 320 with halloysite only. PVA addition increases the interfacial energy, and thus addition of both  
 321 PVA and PEG leads to a similar value, around 15 mN/m. However this value remains low, and  
 322 thus emulsification should be possible with PVA and PVA+PEG.

323

324 Table 1: Oil vs aqueous suspension interfacial energy (at natural pH)

	Interfacial energy (mN/m)
Oil/Water	43 ± 4
Oil/halloysite suspension (5.0 vol.%)	9 ± 2
Oil/halloysite suspension (5.0 vol.%) + PEG 1 wt.%	7 ± 2
Oil/halloysite suspension (5.0 vol.%) + PVA 1 wt.%	15 ± 2
Oil/halloysite suspension (5.0 vol.%) + PVA 1 wt.%+ PEG 1 wt.%	15 ± 2

325

326 The zeta potential of halloysite suspensions was measured with PEG, PVA and PEG+PVA, at  
 327 two pH values: natural pH of 3.4 corresponding to a zeta potential of halloysite suspension  
 328 around -14 mV (Figure 10a), and at pH 7.5 corresponding to a higher zeta potential absolute  
 329 value of halloysite suspension around -43 mV (Figure 10b). By adding PEG of low molecular  
 330 weight, zeta potential is relatively unmodified for the two pH, it attains -10 mV at natural pH,  
 331 and -41 mV at pH 7.5 for 1.5% of PEG. On the contrary, PVA strongly modifies the zeta  
 332 potential of the suspension, which increases at both pH, with a stronger evolution when the  
 333 initial value of the zeta potential is lower (at pH 7.5, Figure 11b). The strongest increase of the  
 334 zeta potential happens at the lowest binder ratio, for 0.2 % of PVA, and then zeta potential  
 335 increases slightly to attain -18 mV at 1.5% of PVA. PVA addition leads to a rapid screening of  
 336 the surface charge of halloysite, i.e. by pushing the shear plane (where the zeta potential is  
 337 measured) further from the particles surface. *When polymers are adsorbed onto the particle  
 338 surface, changes in the ion distribution in the diffuse double layer will affect the absolute zeta  
 339 potential [44][45].* This is similar to cementitious systems where it has been shown that the  
 340 adsorption of such polymeric layers give a significant steric contribution [46].

341

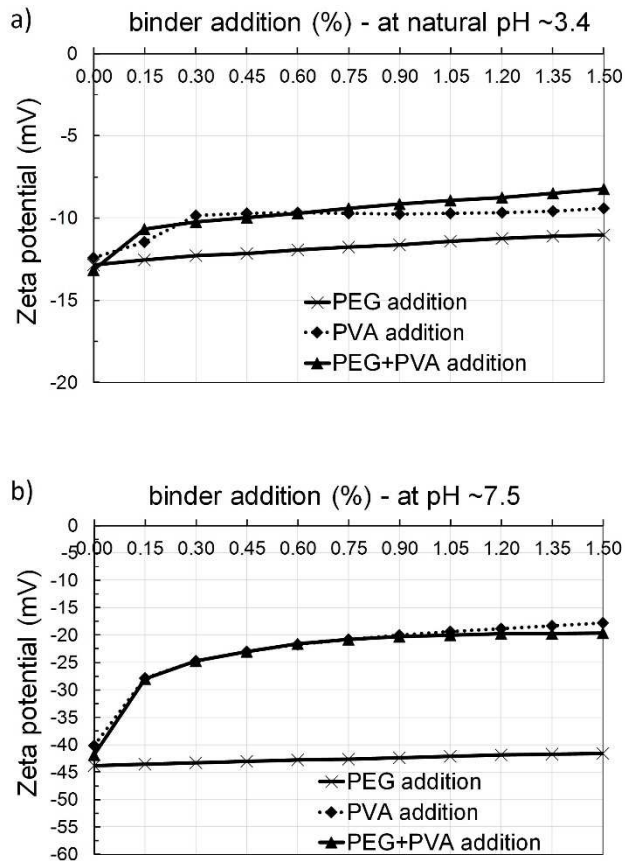
342

343

344

345





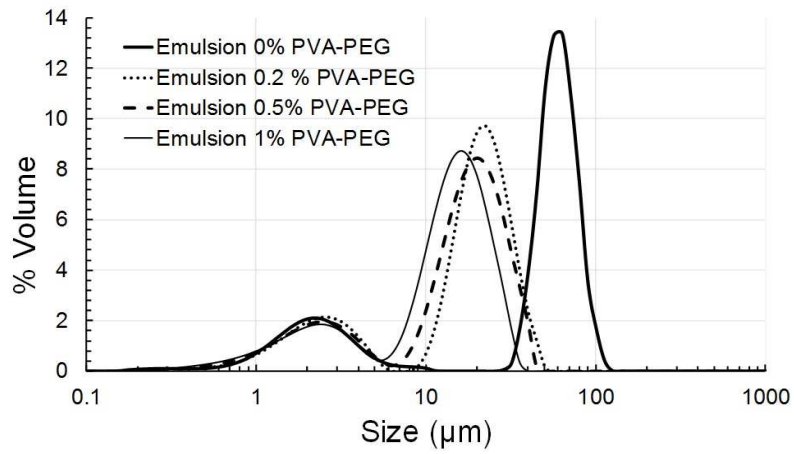
346 Figure 10: Effect of binder addition PVA, PEG and PVA+PEG on zeta potential of an halloysite  
 347 suspension (concentration 5.0 vol.% in deionized water), a) at natural pH 3.4, and b) at pH 7.5

348

349 Then **halloysite emulsions** were prepared from a halloysite suspension at natural pH with  
 350 **different concentrations** of PVA and PEG. These emulsions are composed of smaller droplets,  
 351 between 10 and 30  $\mu\text{m}$  in diameter whereas the mean droplet size was around 70  $\mu\text{m}$  without  
 352 additive as shown by laser diffraction analysis (Figure 11) and optical microscopy (Figure 12).  
 353 The number of droplets is also more important, leading to less particles in the continuous  
 354 phase. These polymers present an amphiphilic character which allow them to adsorb to  
 355 halloysite surfaces via hydrogen bonding, and to increase at the same time the hydrophobicity  
 356 of mineral particles thanks to their carbon chain, leading to a higher emulsification rate.

357

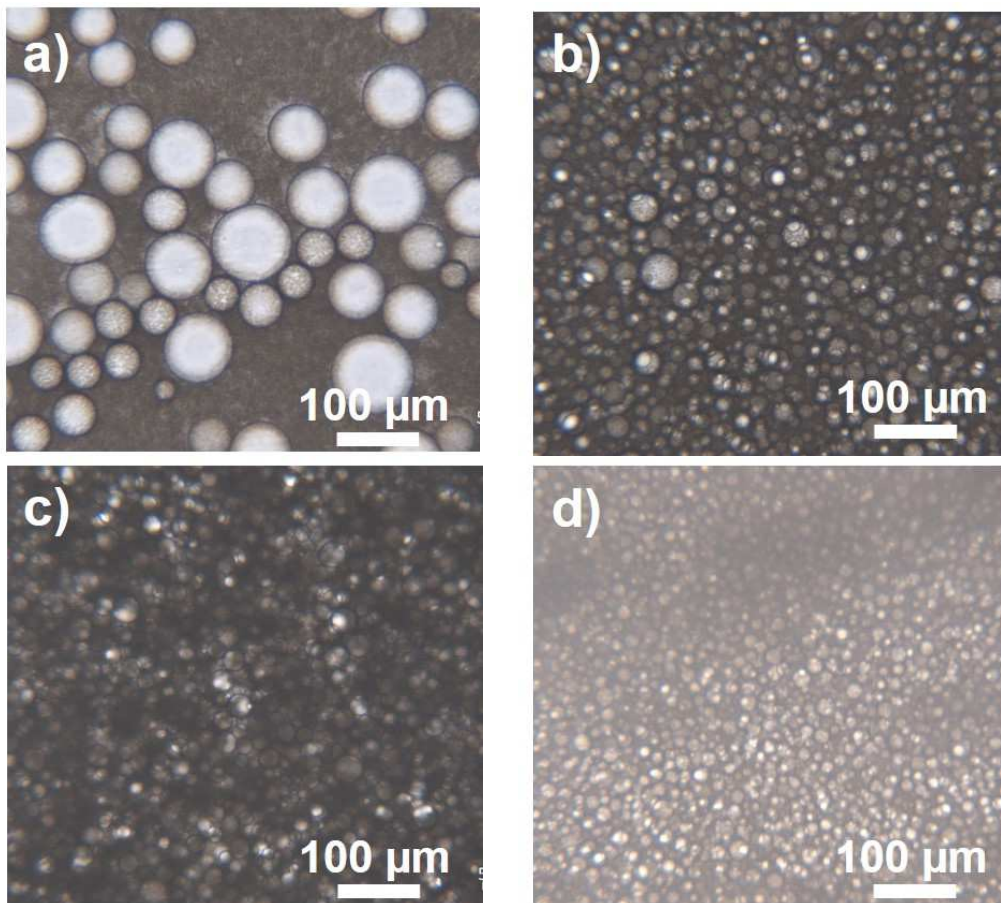




358

359 Figure 11: Laser diffraction analysis of halloysite emulsions from halloysite suspensions at  
 360 natural pH with 0 – 0.2% - 0.5% - 1% PVA and PEG

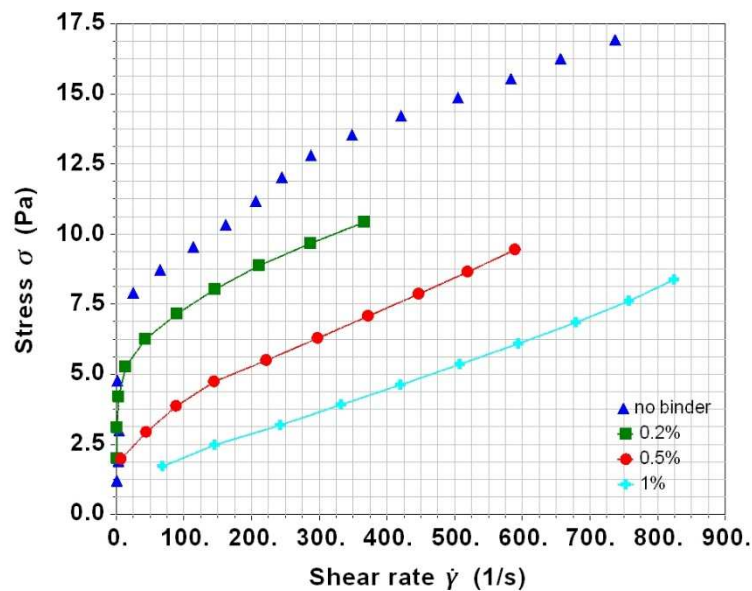
361



362 Figure 12: Optical microscopy of halloysite emulsions at natural pH with a) 0% of PVA and  
 363 PEG, b) 0,2% of PVA and PEG, c) 0,5% of PVA and PEG, d) 1% of PVA and PEG

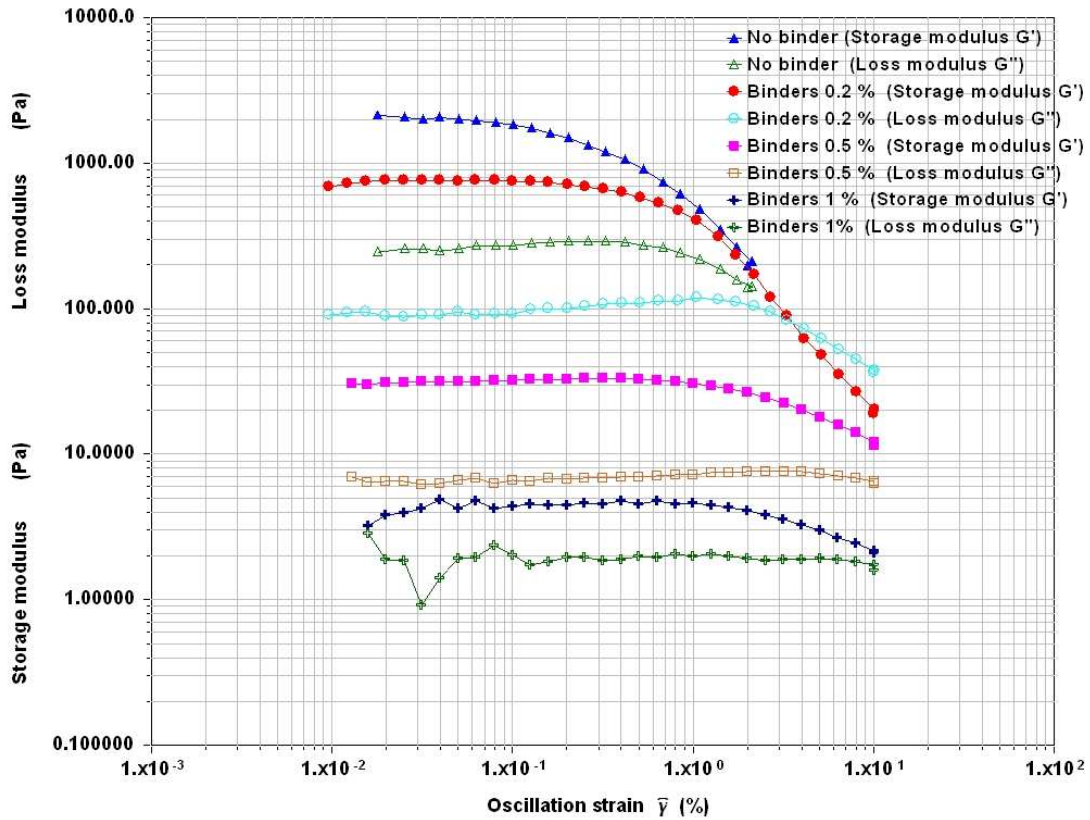
364

365 Figure 13 shows steady state flow rheological experiments of halloysite emulsions with  
 366 different PVA+PEG concentrations. The addition of these organic binders decreases emulsion  
 367 viscosity. The emulsion without dispersant clearly presents a yield stress and a shear thinning  
 368 behavior, whereas the addition of binders decreases the yield stress and leads to a more  
 369 Newtonian flow. Besides, oscillatory measurements (Figure 14) show a very strong decrease  
 370 of the storage modulus  $G'$  by almost three orders of magnitude, as well as the loss modulus  
 371  $G''$ , when adding 1 wt.% of PVA and PEG. Even if  $G'$  still remains higher than  $G''$ ,  
 372 corresponding to a solid-like behavior, the emulsions prepared with binders are more fluid. At  
 373 the same time the critical strain increases with the concentration of binders, therefore these  
 374 emulsions support higher shear stresses. At the end they all present a similar value of their  
 375 cohesive energy around  $0.5 \text{ mJ/m}^3$  considering the large error bars.



376

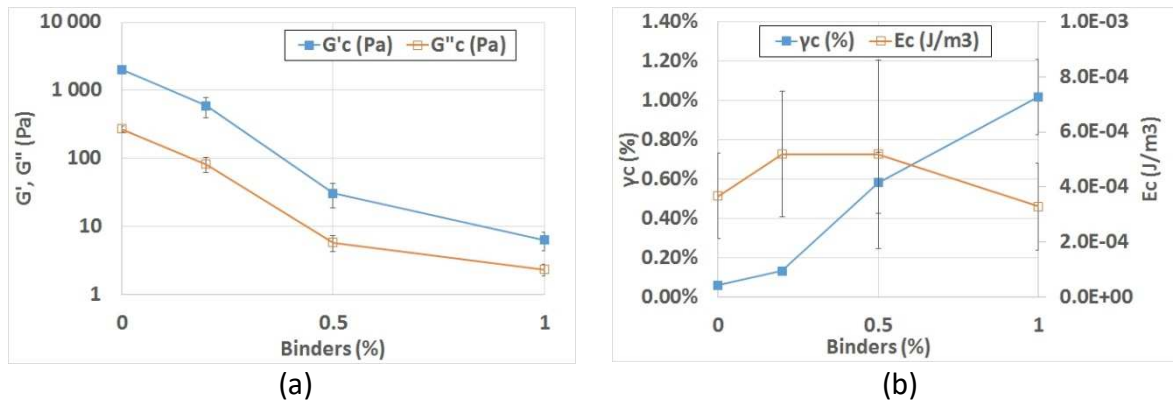
377 Figure 13: Steady state measurements for halloysite emulsions prepared at natural pH with  
 378 different concentrations of PVA and PEG



379

380 Figure 14: Oscillatory measurements for halloysite emulsions prepared at natural pH with  
 381 different concentrations of PVA and PEG

382



383 Figure 15: (a) critical storage modulus  $G'_c$  and critical loss modulus  $G''_c$ , (b) critical strain  $\gamma_c$ ,  
 384 and cohesive energy  $E_c$ , of halloysite emulsions at natural pH with different concentrations of  
 385 PVA and PEG

386

387

388

### 389 3.4- Freeze granulation of emulsions and characterization of halloysite granules

390 The microstructure of powders obtained from freeze granulation of different Pickering  
391 emulsions stabilized with halloysite particles is studied below.

392 Besides their very different rheological behaviors, freeze granulation of emulsions prepared at  
393 different pH (pH 3.4, pH 5 and pH 6) led to granules with similar morphologies: some granules  
394 present a spherical shape as expected from the freeze granulation process, with diameters  
395 are comprised between 50 and 300  $\mu\text{m}$  (Figure 16). Their cohesion is not good, as shown by  
396 the size distribution obtained on the dry granules. Indeed the size distribution is bimodal with  
397 a peak around 1  $\mu\text{m}$  corresponding to halloysite particles, and another mode around 10  $\mu\text{m}$   
398 corresponding to aggregated particles and broken granules. They are very porous as shown  
399 by a closer observation of the surface, broken granules and also from an observation of the  
400 interior of granules, obtained from embedded granules in a resin after being cut and polished  
401 (Figure 16). These pictures exhibit a typical arrangement of halloysite particles, which form  
402 layers, certainly due to the fast freezing in liquid nitrogen, and the lyophilisation step. By  
403 comparing the microstructure of granules obtained from these different emulsions and from a  
404 halloysite suspension, there is no major difference: similar shape, diameter and porosity were  
405 obtained. Therefore we could conclude that Pickering emulsions were certainly broken during  
406 the spraying step. The dispersion of oil droplets was not retained during the process, and the  
407 porosity is mainly due to the relatively low solid fraction used for this process.

408 Freeze granulation of emulsions prepared at pH 3.4 with different concentrations of binders  
409 PVA + PEG led to the granules observed by SEM in Figure 18. All granules present spherical  
410 shape. The size distribution measured on dry granules increases with the concentration of PVA  
411 and PEG (Figure 17). The mode around 1  $\mu\text{m}$  corresponding to halloysite particles has  
412 disappeared from 0.5% of binder, which corresponds to a higher cohesion of the granules.  
413 With the lowest binder concentrations (0.2 and 0.5 %), the surface morphology is close to what  
414 was observed without additive in Figure 16, i.e. a porous structure with layers of halloysite  
415 particles along freezing directions. However when increasing the binder concentration to 1%,  
416 the surface of granules looks smoother and the porosity is more homogeneously distributed.  
417 Contrary to emulsions without binders, typical columnar morphologies due to water elimination  
418 during the sublimation step are not observed. Inside granules some cavities are obtained which  
419 are attributed to the presence of oil droplets in the formulation. Therefore binder addition is  
420 necessary to retain the structure and give enough cohesion. This can be related to the lower  
421 viscosity of these emulsions, as well as their higher critical strain, which allow the conservation  
422 of their internal structure during the spraying step.

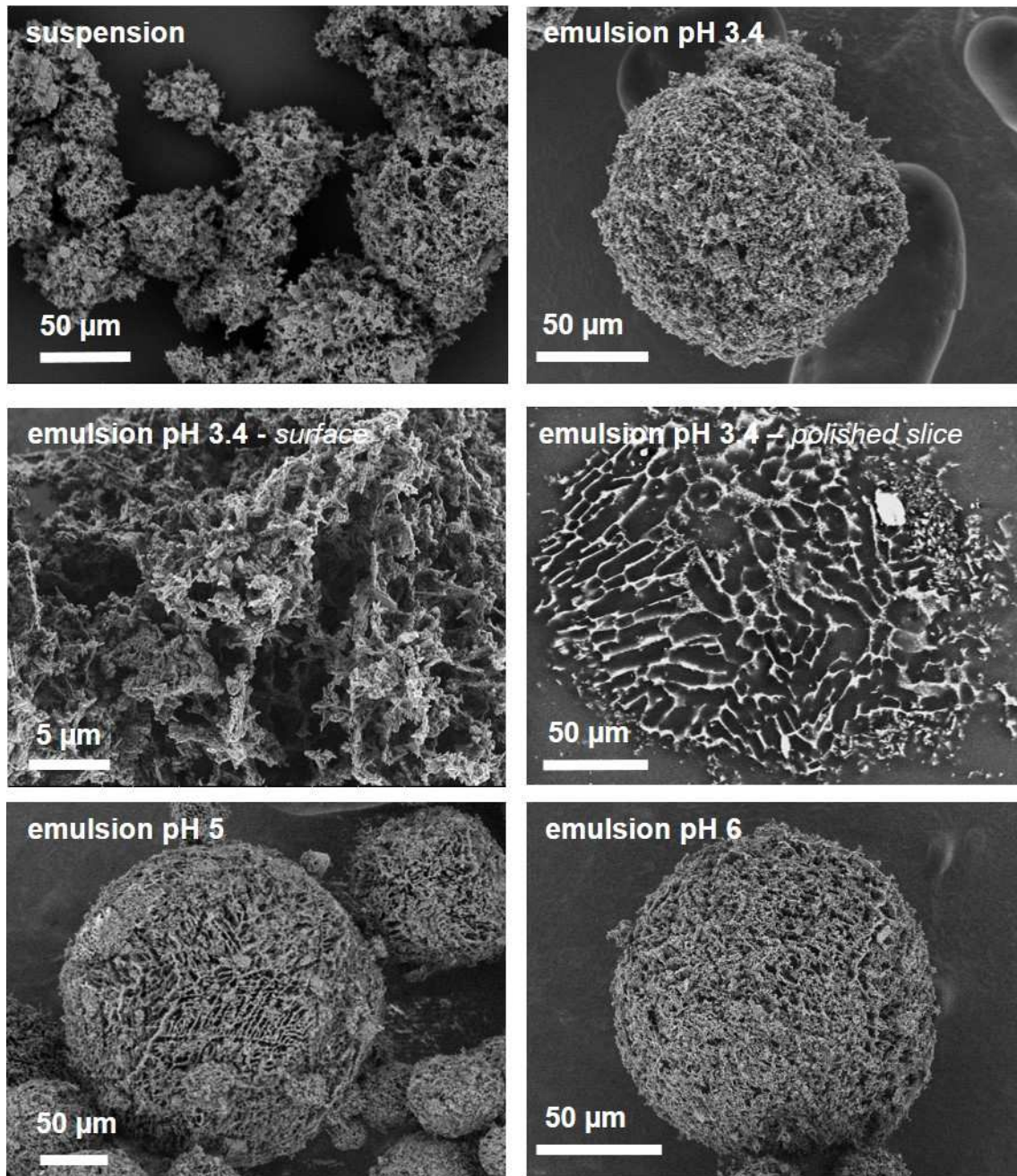
423



424

425

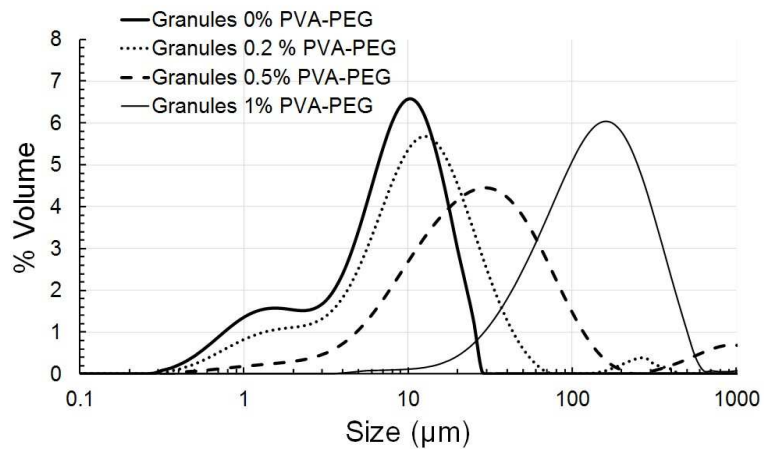
426



427

428 Figure 16: SEM observations of powders obtained by freeze granulation from halloysite

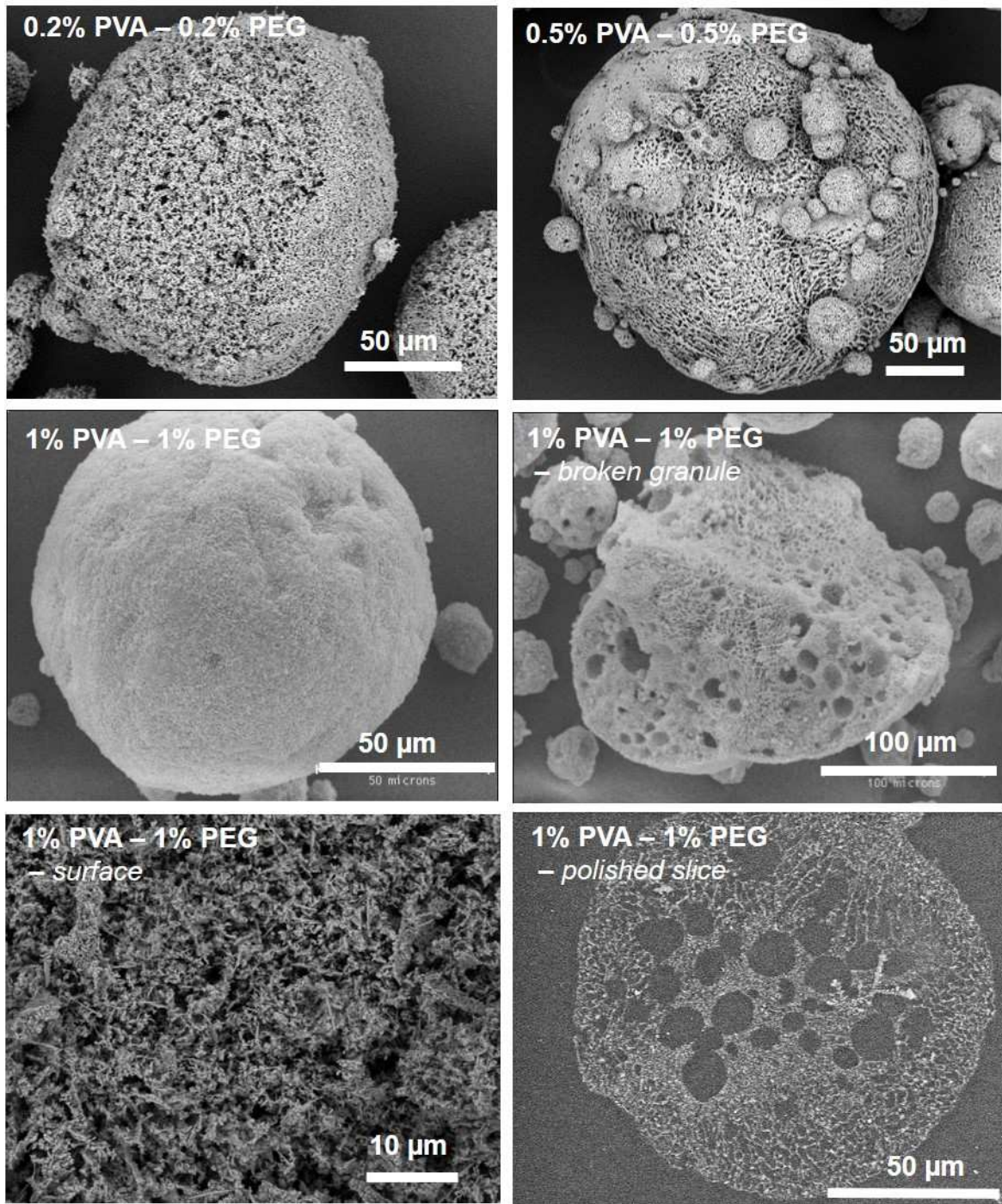
429 suspension and emulsions without binder



430

431 Figure 17: Laser diffraction analysis of granules obtained by freeze granulation of halloysite  
 432 emulsions at natural pH with 0 – 0.2% - 0.5% - 1% PVA and PEG





433

434 Figure 18: SEM observations of powders obtained by freeze granulation from halloysite

435 emulsions with different concentrations of PVA and PEG

436

437

438

439



#### 440 **4- Conclusion**

441 Freeze granulation was applied to Pickering emulsions to prepare porous granules. Halloysite  
442 was chosen on the basis of a former study which has shown halloysite can give stable  
443 Pickering emulsions at a relatively high solid fraction, with an interesting rheological behavior  
444 and a high cohesion. From a fundamental approach, one of the main interesting result from  
445 this study is the exhibition of the strong influence of electrostatic interactions on emulsion  
446 stability, varying the pH and NaCl concentration. In classical Pickering systems hydrophobic  
447 effects have to be considered, which is not the case with a stabilization of O/W emulsions by  
448 clays only. The addition of organic additives led also to stable emulsions, and more importantly  
449 to freeze-dried granules which preserved the emulsion shape. By studying their rheological  
450 behavior, these emulsions showed the lowest viscosity, and the highest critical strain.  
451 Therefore they were able to support higher shear stresses, necessary during the spraying step.  
452 Therefore Pickering emulsions stabilized with clays such as halloysite present very good  
453 performances. These materials are also readily available, cheap and natural resources. They  
454 offer a great opportunity for the development of surfactant-free emulsions that can be used in  
455 large markets such as cosmetics and food products. Moreover by freeze granulation of  
456 Pickering emulsions, porous halloysite granules were obtained, which have a high potential for  
457 the encapsulation of organic substances, or as catalyst supports.

458

#### 459 **Acknowledgement**

460 The authors are grateful to Gilles Gasgnier from Imerys Ceramic Centre (Limoges, France) for  
461 the supply of halloysite powder.

462

#### 463 **References**

- 464 [1] Y. Chevalier and M.-A. Bolzinger, "Emulsions stabilized with solid nanoparticles: Pickering  
465 emulsions," *Colloids Surf. Physicochem. Eng. Asp.*, vol. 439, pp. 23–34, 2013.
- 466 [2] W. Ramsden, "Separation of Solids in the Surface-Layers of Solutions and 'Suspensions'  
467 (Observations on Surface-Membranes, Bubbles, Emulsions, and Mechanical Coagulation). –  
468 Preliminary Account," *Proc. R. Soc. Lond.*, vol. 72, no. 477–486, pp. 156–164, Jan. 1903.
- 469 [3] S. U. Pickering, "CXCVI.—Emulsions," *J. Chem. Soc. Trans.*, vol. 91, no. 0, pp. 2001–2021, Jan.  
470 1907.
- 471 [4] V. B. Menon and D. T. Wasan, "Characterization of oil—water interfaces containing finely  
472 divided solids with applications to the coalescence of water-in-oil Emulsions: A review," *Colloids  
473 Surf.*, vol. 29, no. 1, pp. 7–27, 1988.
- 474 [5] B. P. Binks, "Particles as surfactants—similarities and differences," *Curr. Opin. Colloid Interface  
475 Sci.*, vol. 7, no. 1–2, pp. 21–41, Mar. 2002.

- 476 [6] B. P. Binks and J. H. Clint, "Solid Wettability from Surface Energy Components: Relevance to  
477 Pickering Emulsions," *Langmuir*, vol. 18, no. 4, pp. 1270–1273, 2002.
- 478 [7] R. Aveyard, B. P. Binks, and J. H. Clint, "Emulsions stabilised solely by colloidal particles," *Adv.*  
479 *Colloid Interface Sci.*, vol. 100–102, pp. 503–546, 2003.
- 480 [8] B. P. Binks and S. O. Lumsdon, "Influence of Particle Wettability on the Type and Stability of  
481 Surfactant-Free Emulsions†," *Langmuir*, vol. 16, no. 23, pp. 8622–8631, Nov. 2000.
- 482 [9] G. Lagaly, M. Reese, and S. Abend, "Smectites as colloidal stabilizers of emulsions: I.  
483 Preparation and properties of emulsions with smectites and nonionic surfactants," *Appl. Clay*  
484 *Sci.*, vol. 14, no. 1–3, pp. 83–103, 1999.
- 485 [10] S. Arditty, V. Schmitt, J. Giermanska-Kahn, and F. Leal-Calderon, "Materials based on solid-  
486 stabilized emulsions," *J. Colloid Interface Sci.*, vol. 275, no. 2, pp. 659–664, 2004.
- 487 [11] K. Lebdioua, A. Aimable, M. Cerbelaud, A. Videcoq, and C. Peyratout, "Influence of different  
488 surfactants on Pickering emulsions stabilized by submicronic silica particles," *J. Colloid Interface*  
489 *Sci.*, vol. 520, pp. 127–133, Jun. 2018.
- 490 [12] B. P. Binks, W. Liu, and J. A. Rodrigues, "Novel Stabilization of Emulsions via the  
491 Heteroaggregation of Nanoparticles," *Langmuir*, vol. 24, no. 9, pp. 4443–4446, May 2008.
- 492 [13] M. Cerbelaud, A. Aimable, and A. Videcoq, "Role of Electrostatic Interactions in Oil-in-Water  
493 Emulsions Stabilized by Heteroaggregation: An Experimental and Simulation Study," *Langmuir*,  
494 vol. 34, no. 51, pp. 15795–15803, Dec. 2018.
- 495 [14] S. Abend, N. Bonnke, U. Gutschner, and G. Lagaly, "Stabilization of emulsions by  
496 heterocoagulation of clay minerals and layered double hydroxides," *Colloid Polym. Sci.*, vol.  
497 276, no. 8, pp. 730–737, Sep. 1998.
- 498 [15] Y. Nonomura and N. Kobayashi, "Phase inversion of the Pickering emulsions stabilized by plate-  
499 shaped clay particles," *J. Colloid Interface Sci.*, vol. 330, no. 2, pp. 463–466, 2009.
- 500 [16] G. Lagaly, M. Reese, and S. Abend, "Smectites as colloidal stabilizers of emulsions: II.  
501 Rheological properties of smectite-laden emulsions," *Appl. Clay Sci.*, vol. 14, no. 5–6, pp. 279–  
502 298, 1999.
- 503 [17] N. P. Ashby and B. P. Binks, "Pickering emulsions stabilised by Laponite clay particles," *Phys.*  
504 *Chem. Chem. Phys.*, vol. 2, no. 24, pp. 5640–5646, 2000.
- 505 [18] B. Rotenberg, "Modélisation multi-échelles du comportement de l'eau et des ions dans les  
506 argiles," PhD Thesis, Université Pierre et Marie Curie - Paris VI, 2007.
- 507 [19] D. Kpogbemabou, G. Lecomte-Nana, A. Aimable, M. Bienia, V. Niknam, and C. Carrion, "Oil-in-  
508 water Pickering emulsions stabilized by phyllosilicates at high solid content," *Colloids Surf.*  
509 *Physicochem. Eng. Asp.*, vol. 463, pp. 85–92, 2014.
- 510 [20] K. Rundgren, O. Lyckfeldt, and M. Sjostedt, "Improving Powders With Freeze Granulation,"  
511 *Ceramic Industry*, vol. 153, pp. 40–44, 2003.
- 512 [21] W. J. J. Walker, J. S. Reed, and S. K. Verma, "Influence of Slurry Parameters on the  
513 Characteristics of Spray-Dried Granules," *J. Am. Ceram. Soc.*, vol. 82, no. 7, pp. 1711–1719,  
514 1999.
- 515 [22] E. Lintingre, F. Lequeux, L. Talini, and N. Tsapis, "Control of particle morphology in the spray  
516 drying of colloidal suspensions," *Soft Matter*, vol. 12, no. 36, pp. 7435–7444, Sep. 2016.
- 517 [23] S. Shanmugam, "Granulation techniques and technologies: recent progresses," *BiolImpacts*, vol.  
518 5, no. 1, pp. 55–63, Aug. 2017.
- 519 [24] M. Stuer, Z. Zhao, and P. Bowen, "Freeze granulation: Powder processing for transparent  
520 alumina applications," *J. Eur. Ceram. Soc.*, vol. 32, no. 11, pp. 2899–2908, Aug. 2012.
- 521 [25] M. Stuer and P. Bowen, "Yield stress modelling of doped alumina suspensions for applications  
522 in freeze granulation: towards dry pressed transparent ceramics," *Adv. Appl. Ceram.*, vol. 111,  
523 no. 5–6, pp. 254–261, Aug. 2012.
- 524 [26] F. La Lumia, L. Ramond, C. Pagnoux, and G. Bernard-Granger, "Fabrication of homogenous  
525 pellets by freeze granulation of optimized TiO<sub>2</sub>-Y<sub>2</sub>O<sub>3</sub> suspensions," *J. Eur. Ceram. Soc.*, vol. 39,  
526 no. 6, pp. 2168–2178, Jun. 2019.

- 527 [27] O. Lyckfeldt, K. Rundgren, and M. Sjöstedt, "Freeze Granulation for the Processing of Silicon  
528 Nitride Ceramics," *Key Eng. Mater.*, 2004.
- 529 [28] Q. Wang, S. M. Olhero, J. M. F. Ferreira, W. Cui, K. Chen, and Z. Xie, "Hydrolysis Control of AlN  
530 Powders for the Aqueous Processing of Spherical AlN Granules," *J. Am. Ceram. Soc.*, vol. 96, no.  
531 5, pp. 1383–1389, 2013.
- 532 [29] P. Barick, B. P. Saha, S. V. Joshi, and R. Mitra, "Spray-freeze-dried nanosized silicon carbide  
533 containing granules: Properties, compaction behaviour and sintering," *J. Eur. Ceram. Soc.*, vol.  
534 36, no. 16, pp. 3863–3877, Dec. 2016.
- 535 [30] A. R. Studart, U. T. Gonzenbach, E. Tervoort, and L. J. Gauckler, "Processing Routes to  
536 Macroporous Ceramics: A Review," *J. Am. Ceram. Soc.*, vol. 89, no. 6, pp. 1771–1789, 2006.
- 537 [31] I. Akartuna, A. R. Studart, E. Tervoort, and L. J. Gauckler, "Macroporous Ceramics from Particle-  
538 stabilized Emulsions," *Adv. Mater.*, vol. 20, no. 24, pp. 4714–4718, 2008.
- 539 [32] I. Lesov, S. Tcholakova, M. Kovadjieva, T. Saison, M. Lamblet, and N. Denkov, "Role of Pickering  
540 stabilization and bulk gelation for the preparation and properties of solid silica foams," *J.*  
541 *Colloid Interface Sci.*, vol. 504, pp. 48–57, Oct. 2017.
- 542 [33] J. A. Lewis, J. E. Smay, J. Stuecker, and J. Cesarano, "Direct Ink Writing of Three-Dimensional  
543 Ceramic Structures," *J. Am. Ceram. Soc.*, vol. 89, no. 12, pp. 3599–3609, 2006.
- 544 [34] M. A. Torres Arango, N. J. Morris, and K. A. Sierros, "Direct Writing and Controlling of  
545 Hierarchical Functional Metal-Oxides: Bio-inspired Multiphase Processing, 3D Printing and  
546 Hierarchical Cellular Structuring," *JOM*, vol. 70, no. 9, pp. 1823–1829, 2018.
- 547 [35] L. Alison *et al.*, "3D printing of sacrificial templates into hierarchical porous materials," *Sci. Rep.*,  
548 vol. 9, no. 1, 2019.
- 549 [36] R. Kamble, M. Ghag, S. Gaikwad, and B. K. Panda, "Halloysite Nanotubes and Applications: A  
550 Review," *J. Adv. Sci. Res.*, vol. 3, no. 2, pp. 25–29, 2012.
- 551 [37] P. Yuan, D. Tan, and F. Annabi-Bergaya, "Properties and applications of halloysite nanotubes:  
552 Recent research advances and future prospects," *Appl. Clay Sci.*, vol. 112–113, pp. 75–93, 2015.
- 553 [38] G. Lazzara *et al.*, "An assembly of organic-inorganic composites using halloysite clay  
554 nanotubes," *Curr. Opin. Colloid Interface Sci.*, vol. 35, pp. 42–50, 2018.
- 555 [39] N. Gabas, N. Hiquily, and C. Laguérie, "Response of Laser Diffraction Particle Sizer to  
556 Anisometric Particles," *Part. Part. Syst. Character.*, vol. 11, no. 2, pp. 121–126, 1994.
- 557 [40] E. Chibowski, A. E. Wiacek, L. Holysz, and K. Terpilowski, "Investigation of the Electrokinetic  
558 Properties of Paraffin Suspension. 1. In Inorganic Electrolyte Solutions," *Langmuir*, vol. 21, no.  
559 10, pp. 4347–4355, May 2005.
- 560 [41] M. Cerbelaud, A. Videcoq, L. Alison, E. Tervoort, and A. R. Studart, "Early Dynamics and  
561 Stabilization Mechanisms of Oil-in-Water Emulsions Containing Colloidal Particles Modified  
562 with Short Amphiphiles: A Numerical Study," *Langmuir*, vol. 33, no. 50, pp. 14347–14357, Dec.  
563 2017.
- 564 [42] M. Donnet, P. Bowen, and J. Lemaître, "A thermodynamic solution model for calcium  
565 carbonate: Towards an understanding of multi-equilibria precipitation pathways," *J. Colloid*  
566 *Interface Sci.*, vol. 340, no. 2, pp. 218–224, Dec. 2009.
- 567 [43] J. S. Reed, *Principles of Ceramics Processing*. Wiley, 1995.
- 568 [44] A. U. Khan, B. J. Briscoe, and P. F. Luckham, "Interaction of binders with dispersant stabilised  
569 alumina suspensions," *Colloids Surf. Physicochem. Eng. Asp.*, vol. 161, no. 2, pp. 243–257, Jan.  
570 2000.
- 571 [45] J. Ma, R. Zhang, C. H. Liang, and L. Weng, "Colloidal characterization and electrophoretic  
572 deposition of PZT," *Mater. Lett.*, vol. 57, no. 30, pp. 4648–4654, Dec. 2003.
- 573 [46] M. Palacios *et al.*, "Repulsion forces of superplasticizers on ground granulated blast furnace slag  
574 in alkaline media, from AFM measurements to rheological properties," *Mater. Construcción*,  
575 vol. 62, no. 308, pp. 489–513, 2012.
- 576